Experimental Hematology

Experimental Hematology 2019;72:47–59

Sphingosine-1-phosphate signaling modulates terminal erythroid differentiation through the regulation of mitophagy

Chong Yang[a], Michihiro Hashimoto[b], Quy Xiao Xuan Lin[a], Darren Qiancheng Tan[a], and Toshio Suda[a,b]

[a]*Cancer Science Institute, Yong Loo Lin School of Medicine, National University of Singapore, Singapore, Singapore;* [b]*Kumamoto University, International Research Center for Medical Sciences, Kumamoto, Japan*

(Received 17 September 2018; revised 10 January 2019; accepted 11 January 2019)

Erythropoiesis is a highly coordinated stepwise process involving the progressive clearance of mitochondria via mitophagy. Based on the expression of several macroautophagy and mitophagy specific genes, we identified a sequential change in the transcriptional pattern during terminal erythroid differentiation. Because erythroid cells are a major source of serum sphingosine-1-phosphate, we analyzed the role of sphingolipid signaling in erythropoiesis and demonstrate that sphingosine kinase activity promotes terminal erythroid differentiation by regulating the expression of key mitophagy genes Pink1 and Bnip3l/Nix. Sphingosine kinase 1 (Sphk1) inhibition also disrupted Pink1-p62 mediated mitochondria clearance in late erythroblasts. Notably, we show that supplementing sphingosine-1-phosphate in vitro can promote erythroid differentiation. Our study clarifies the role of sphingolipid signaling in regulating mitophagy during terminal erythroid differentiation and highlights the potential utility of modulating sphingolipid signaling to facilitate the large-scale production of transfusable red blood cells. © 2019 Published by Elsevier Inc. on behalf of ISEH – Society for Hematology and Stem Cells.

Erythropoiesis, the process of differentiation from hematopoietic/stem progenitor cells (HSPCs) to mature red blood cells (RBCs), is responsible for the daily production of $\sim 2 \times 10^{11}$ RBCs to maintain homeostatic oxygen supply to various tissues [1,2]. Adult erythropoiesis occurs in the bone marrow (BM) via three stages: early erythropoiesis, terminal erythroid differentiation, and reticulocyte maturation [1,3]. Early erythropoiesis involves the differentiation of HSPCs into megakaryocyte–erythroid progenitors (MEPs), followed by burst-forming unit-erythroid cells, colony-forming unit-erythroid (CFU-E) cells and finally pro-erythroblasts [4]. Terminal erythroid differentiation consists of a stepwise transition from proerythroblasts to basophilic erythroblasts, polychromatic erythroblasts, orthochromatic erythroblasts, and finally enucleated reticulocytes, which degrade their intracellular organelles to become mature RBCs. A well-recognized stimulus of terminal erythroid differentiation is erythropoietin (EPO), which drives the proliferation and differentiation of erythroblasts and prevents apoptosis [5]. However, apart from EPO, few other factors that promote terminal erythroid differentiation have been identified. Therefore, there remains a need to identify factors that regulate terminal erythroid differentiation to facilitate the large-scale in vitro production of transfusable RBCs for clinical use.

During terminal erythroid differentiation, clearance of intracellular organelles occurs during erythroblast maturation into fully functional RBCs [6]. In particular, the selective clearance of mitochondria, termed mitophagy, is known to be an essential biological process for RBC maturation [7]. Key regulators of mitophagy include PTEN-induced putative kinase 1 (PINK1) and the E3 ubiquitin ligase PARKIN, which interact on the outer mitochondrial membrane to facilitate mitochondria aggregation and autophagosome formation [8,9]. In addition, the macroautophagy components Atg5 and Atg7 have also been shown to mediate canonical mitophagy; aberrant accumulation of mitochondria during terminal erythroid differentiation was

Author contributions: TS and CY designed the project, analyzed the data, and wrote the manuscript. MH conducted Atg7 knock-out mice erythroid lineage analysis. QXXL performed RNA-seq analysis of the available transcriptome studies. DQT participated in the writing of manuscript and discussed and analyzed experiments. All authors read and approved the final manuscript.

Offprint requests to: Toshio Suda, MD, Cancer Science Institute, Yong Loo Lin School of Medicine, National University of Singapore, MD6, 12-01, Singapore 117599; Tel: +65 65161155; Fax: 68739664; E-mail: csits@nus.edu.sg

0301-472X/
https://doi.org/10.1016/j.exphem.2019.01.004

reported in *Atg7*-deficient mice [10,11]. Interestingly, Atg5- or Atg7-depleted erythroid cells are still able to induce mitophagy and form autophagosomes independently of LC3 lipidation, but this is dependent on Beclin1, Ulk1, and *Bnip3l/Nix* [12–15], suggesting that mitophagy during terminal erythroid differentiation also involves an Atg5- and Atg7-independent mode of mitophagy [16].

Recent studies have highlighted the potential molecular crosstalk among mitophagy, autophagy, and sphingosine signaling [17]. Autophagy and cell fate are highly interconnected biological processes that share many key regulators [18]. Similarly, sphingolipids differentially regulate cell fate due to the disparate nature of pro-apoptotic ceramide and sphingosine, as well as prosurvival sphingosine-1-phosphate (S1P) [19]. Within the hematopoietic system, RBCs exhibit elevated sphingosine kinase (Sphk) activity, which generates the bioactive lipid S1P from sphingosine [20–23]. Distinct genes encode two Sphk isoforms, Sphk1 and Sphk2, which differ in their biochemical properties, subcellular localization, and function [21,24]. In RBCs, Sphk1 is the predominant isoform and previous observations suggest that S1P synthesis may be regulated in erythrocytes in response to changes in plasma S1P levels [25]. In addition, RBCs are essential sources of S1P that regulate embryonic vascular development during embryogenesis [26]. However, the relationship between sphingosine signaling and mitophagy in the context of terminal erythroid differentiation remains unknown. Moreover, the role of S1P and sphingolipid signaling in adult erythropoiesis remains to be clarified. Therefore, using primary BM and erythroblast cell line models of erythropoiesis, we sought to investigate how S1P regulates terminal erythroid differentiation. Here, we uncover the importance of S1P-mediated signaling in erythropoiesis and present evidence that S1P-mediated signaling regulates terminal erythroid differentiation by modulating mitophagy.

Methods

Mice

Mice used in this study were in the C57/BL6 background. They were used for experiments at 8 to 12 weeks of age. PhAM^{excised} mice were obtained from The Jackson Laboratory. All mice are maintained under experimental protocols approved by institutional animal care and use committees under the National University of Singapore. *Atg7*$^{fl/fl}$*; Mx1Cre* mice were generated at Kumamoto University by crossing *Atg7*$^{fl/fl}$ mice with *Mx1-Cre*-transgenic mice. *Mx1-cre* was induced by two intraperitoneal injections of polyinosine-polycytidylic acid (200 mg/kg) into 4-week-old mice, which were euthanized for experiments 4 weeks after induction. All animal experiments were approved by Kumamoto University and carried out according to the guidelines of Kumamoto University.

Chemicals

The Sphk1 inhibitor Sk1-I was from Enzo Life Sciences (BML-EI411-0005) and diluted in dimethylsulfoxide. Exogenous S1P (D-erythro-sphingosine-1-phosphate) was from Avanti. For exogenous S1P treatment assays, 1 mmol/L stock sphingosine was dissolved in ethanol.

Cell culture

The MEDEP-BRC5 cell line was purchased from RIKEN BioResource Center, Japan. Cells were cultured in Iscove's modified Dulbecco's medium (IMDM) (2 mmol/L L-glutamine) supplemented with 15% fetal bovine serum (FBS), Insulin-transferrin-selenium liquid media supplement (Sigma-Aldrich), 0.45 mmol/L α-monothioglycerol (Sigma-Aldrich), 50 ng/mL mouse stem cell factor (SCF) (PeproTech), 1 μmol/L dexamethasone, and 50 μg/mL ascorbic acid (Sigma-Aldrich).

In vitro liquid culture assays for primary BM cells

BM cells were collected from tibia and femur and subsequently treated with RBC lysis buffer to deplete erythrocytes. RBC depleted BM cells were treated with CD117 microbeads (Miltenyi Biotec), and the CD117-positive population was separated out with the autoMACS Pro Separator (Miltenyi Biotec) following the manufacturer's instructions, and cells were cultured in IMDM supplemented with 10% FBS, SCF (PeproTech), and EPO (BD Biosciences).

shRNA knock-down studies

For short hairpin RNA (shRNA) knock-down studies, the mouse SphK1 (mSphK1)-targeting shRNA, which included an enhanced green fluorescent protein (EGFP) reporter (pLV [shRNA]-EGFP-U6>mSphk1[shRNA#4]), was obtained from Vectorbuilder (Santa Clara, CA).

Antibodies for fluorescence-activated cell sorting and immunostaining

Primary antibodies used for flow cytometry were as follows: c-Kit (2B8, eBioscience), Sca-1 (E13-161.7, BioLegend), TER-119 (Ter119, BD Biosciences), CD71 (C2, BD Biosciences), CD44 (IM7, BD Biosciences), CD34 (RAM34, BD Biosciences), CD16/32 (93, eBioscience), interleukin-7 receptor-alpha (SB/199, BioLegend), CD4 (L3T4, BD Biosciences), CD8 (53-6.72, BD Biosciences), B220 (RA3-6B2, BD Biosciences), Gr-1 (RB6-8C5, BD Biosciences), and Mac-1 (M/70, BD Biosciences). Primary antibodies used for immunofluorescence staining were as follows: rabbit polyclonal anti-PINK1 (ab23707, Abcam) and mouse monoclonal anti-SQSTM1/p62 antibody (ab56416, Abcam). Secondary antibodies were conjugated with Alexa Fluor 555 (red) and Alexa Fluor 647 (magenta) (both from Invitrogen).

Flow cytometry analysis of erythroid populations

Flow cytometric cell sorting was performed using a FACSAria II cell sorter (BD Biosciences) and analyzed using the FlowJo software package (TreeStar). Procedures of isolation and staining of Lin$^-$Sca1$^+$c-Kit$^+$ cells and progenitors were as described previously [27]. Erythroblast isolation from BM was analyzed as follows. Briefly, BM cells were collected from tibias and femurs and stained without RBC lysis.

Erythroid cells were first treated with Fcblock (CD16/CD32, BD Biosciences) and subsequently stained with phycoerythrin-conjugated CD44 and allophycocyanin-conjugated-Ter119. Ter119^{high} populations were further separated into various stages of erythroblasts by CD44 versus forward scatter. Hoechst staining was used to identify and exclude dead cells. Erythroid maturation was analyzed by the staining of CD71 and Ter119.

Tetramethyl-rhodamine ethyl ester mitochondrial membrane potential assay

The mitochondrial membrane potential was analyzed from the staining of tetramethyl-rhodamine ethyl ester (TMRE; Enzo) following the manufacturer's instructions. Briefly, cells were treated with TMRE at a final concentration of 5 μmol/L for 30 minutes at 37°C. The cells were further treated with Fcblock and stained with a Ter119 and CD44 FACS antibody. The fluorescent intensities of TMRE were measured by flow cytometry.

MitoTracker Green mitochondria content assay

The mitochondrial content was analyzed with staining from MitoTracker Green (MTG; Thermo Fisher Scientific) following the manufacturer's instructions. Briefly, cells were treated with MTG at a final concentration of 5 μmol/L for 30 minutes at 37°C. The cells were further treated with Fcblock and stained with a Ter119 and CD44 FACS antibody. The fluorescent intensities of MTG were measured by flow cytometry.

Intracellular reactive oxygen species level detection assay

The intracellular reactive oxygen species (ROS) level was analyzed with the CellROX Deep Red probe (Thermo Fisher Scientific) according to the manufacturer's instructions. Briefly, cells were treated with CellROX at a final concentration of 5 μmol/L for 30 minutes at 37°C. The cells were further treated with Fcblock and stained with a Ter119 and CD44 FACS antibody. The fluorescent intensities of CellROX were measured by flow cytometry.

Immunostaining and confocal microscopy

Cultured erythroblasts (Ter119^{+}/CD71^{-}) were sorted onto the slides, followed by 4% paraformaldehyde fixation and 0.25% Triton X-100 permeabilization. Cells were subsequently incubated in Protein Block Serum-Free reagent (Dako X0909) at room temperature for 1 hour. and then subjected to immunofluorescence staining using standard protocols. For the PINK1/p62/mito-dendra2 colocalization experiment, PermaFluor Aqueous Mounting Medium from Thermo Fisher Scientific was used to enhance fluorescein isothiocyanate intensity.

Fluorescence images were obtained using an A1R HD (Nikon) following the manufacturer's instructions. Images obtained from various erythroblasts were analyzed using NIS Elements software (Nikon).

RNA extraction and quantitative real-time polymerase chain reaction

Total RNA was extracted and purified with the RNeasy kit (Qiagen). Subsequently, total RNA was reverse transcribed to cDNA using the SuperScript IV VILO Master Mix (Thermo Fisher Scientific) following the manufacturer's instructions. Quantitative real-time polymerase chain reaction (qRT-PCR) was performed using SYBR green master mix (Thermo Fisher Scientific, A25742). Data were collected and analyzed on a QuantStudio 3 (Thermo Fisher Scientific). Gapdh and Hprt housekeeping genes were used to normalize samples.

Table 1 shows the primers that were used.

Table 1. List of primer sequences used for RT-PCR analysis in this study

Primer name	Primer sequence(5′-3′)
mSphk1-F	ACCTTTAAACTGATACTCACCGAAC
mSphk1-R	GACCATCACCGGACATGACT
mAtg5-F	GCAGAATGACAGATTTGACCAG
mAtg5-R	AGCTTCTGGATGAAAGGCC
mAtg7-F	TTGACATGAGTGCCTCCAC
mAtg7-R	ACCTGACTTTATGGCTTCCC
mPink1-F	GACTCCCACCTTTCCCTTTG
mPink1-R	GTAACTGCTCCATACTCTCCAG
mNix-F	TCTTCCTTTCTCATGTGCTGG
mNix-R	GCTTTTCGTCTCCCTCAGTAG
mGapdh-F	CTTTGTCAAGCTCATTTCCTGG
mGapdh-R	TCTTGCTCAGTGTCCTTGC
mHprt-F	GCCTAAGATGAGCGCAAGTTG
mHprt-R	TACTAGGCAGATGGCCACAGG

F=forward; R=reverse.

RNA-sequencing data extraction and analysis

Processed RNA-sequencing (RNA-seq) datasets in four stages of murine terminal erythroid differentiation generated by An et al. [28] were downloaded from the Gene Expression Omnibus (GEO) datasets (GEO accession: GSE53983). RNA-seq raw reads were aligned to the murine mm9 genome using TopHat with default parameters [29] and aligned reads in every gene were counted using htseq-count [30]. Reads per kilobase of transcript per million mapped reads was used as a normalized measure of gene expression.

Statistical analysis

All results were performed at least three times independently under similar conditions. Statistical significance was calculated using two-tailed unpaired t tests; $p < 0.05$ was considered statistically significant.

Results

Dynamic changes in functional mitochondria content occur during terminal erythroid differentiation

We identified different stages of terminal erythroid differentiation by flow cytometry using a combination of cell size (i.e., forward scatter) and expression levels of Ter119 and CD44. Consistent with prior observations [31], we confirmed the presence of proerythroblasts, basophilic erythroblasts (I), polychromatic erythroblasts (II), orthochromatic erythroblasts (III), and reticulocytes (IV) in murine BM (Figure 1A).

To assess mitochondrial content during terminal erythroid differentiation, we first quantified the mitochondrial mass and activity of mitochondria at each differentiation

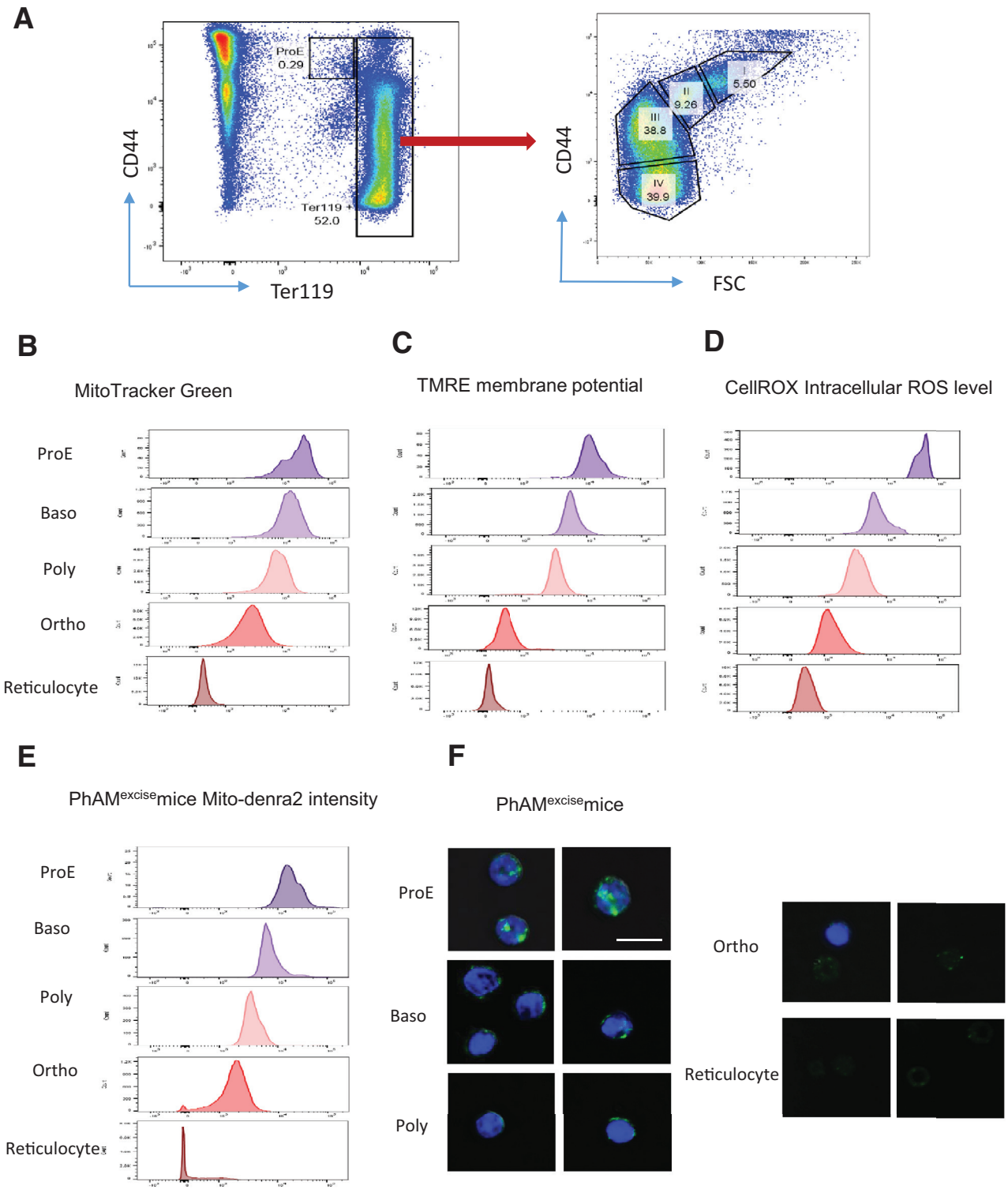

Figure 1. Dynamic changes in mitochondria content and activity during terminal erythroid differentiation. **(A)** Representative flow cytometric plots showing the gating of erythroid populations based on Ter119 and CD44 expression. **(B)** MTG staining of various erythroid populations. **(C)** TMRE staining of various erythroid populations. **(D)** CellRox staining of various erythroid populations. **(E,F)** Dendra2 fluorescence intensity of various erythroid populations isolated from PhAM^{excise} mice as determined by **(E)** flow cytometry and **(F)** confocal imaging. Scale bars, 20 μm. Data shown are representative of three independent experiments.

stage. Using MTG and TMRE staining, we observed a progressive reduction in the mass (Figure 1B) and activity (Figure 1C) of mitochondria with differentiation. Notably, we observed a prominent reduction in mitochondrial activity between the proerythroblast and basophilic erythroblast stages, as well as the polychromatic erythroblast and reticulocyte stages (Figure 1C). Importantly, this decrease in mitochondrial activity correlated with a similarly progressive decrease in intracellular ROS levels (Figure 1D), consistent with the current opinion that erythroid progenitors metabolically switch from oxidative phosphorylation to glycolysis to meet energy demands during differentiation [32]. Therefore, our observations confirm that terminal erythroid differentiation involves a stepwise reduction in mitochondrial activity.

Because MTG staining might be influenced by the efflux capacity of erythroid cells [33], we employed PhAM^{excised} mice, which ubiquitously express mitochondrial-specific Dendra2 monomeric fluorescent protein that serves as a robust indicator of mitochondria content [34]. In agreement with the MTG and TMRE results (Figures 1B and 1C), Dendra2 fluorescence intensity decreased with differentiation, particularly between the proerythroblast and basophilic erythroblast stages and the polychromatic erythroblast and reticulocyte stages (Figure 1E). Using confocal microscopy, we likewise confirmed the decrease in Dendra2 intensity, which coincides with enucleation at the polychromatic erythroblast stage (Figure 1F), suggesting that the decrease in mitochondrial activity is due to the reduction in the content of functional mitochondria. Therefore, terminal erythroid differentiation is closely associated with a decrease in mitochondria content.

Sequential changes of the macroautophagy and mitophagy gene expression occur during terminal erythroid maturation

We next clarified the underlying mechanism mediating clearance of functional mitochondria. To do so, we first analyzed the transcriptome of murine erythroblasts at various stages of terminal differentiation using RNA-seq data previously obtained [28]. Interestingly, we observed that macroautophagy factors (e.g., *Atg3, Atg5, Atg7*, and *Atg10*) and several mediators of mitophagy (e.g., *Pink1, Park2, Bnip3l/Nix*, and *P62/Sqstm1*) were expressed in a distinct, inversely correlated pattern that coincided with erythroblast maturation stage (Figure 2A). For instance, the macroautophagy genes *Atg5* and *Atg7* were highly expressed in the early stage of terminal erythroid differentiation and gradually downregulated with erythroblast maturation (Figure 2A). In contrast, expression of the mitophagy-specific genes Pink1 and Nix/Bnip3L increased with erythroblast maturation and peaked at the orthochromatic erythroblast stage. The expression patterns of these genes (*Atg5, Atg7, Pink1*, and *Nix*) were further validated by qRT-PCR (Figure 2B). Functional mitochondria content (Figure 1) correlated positively with *Atg5* and *Atg7* expression, but correlated inversely with Nix and Pink1 expression.

Consistent with these observations, terminal erythropoiesis was only partially affected in ATG7-deficient mice (*Atg7*$^{fl/fl}$*;Mx1-Cre* mice), which exhibited a partial decrease in the proportion of late erythroblasts/reticulocytes (Ter119 single positive) and early erythroblasts (Ter119/CD71 double positive; Figure 2C). These observations suggest that mitochondria clearance is distinctly regulated during the early and late stages of terminal erythroid differentiation.

SPHK1 activity is required for terminal erythroid differentiation in vitro

We next sought to uncover novel autophagic regulators of terminal erythroid differentiation, and the reported role of sphingosine signaling in autophagy regulation and its relation to RBCs drew our attention [17,23,25]. We first assessed the expression level of *Sphk1* at various stages of terminal erythroid differentiation. Consistent with the high SPHK1 activity reported in RBCs [25], we observed high *Sphk1* expression from the MEP phase onward and throughout terminal erythroid differentiation (Figure 3A).

We then determined the functional relevance of SPHK1 and its product (S1P) at various stages of terminal erythroid differentiation using a murine primary BM cell culture model of erythropoiesis. In addition, we used the mouse embryonic stem cell (BRC5)-derived erythroid progenitor cell line MEDEP-BRC5 as an alternative model to facility subsequent investigation. The MEDEP-BRC5 line was established by Hiroyama et al., RIKEN BioResource Center, Japan, and exhibits characteristics of early erythroblasts with the capability of differentiating into enucleated RBCs [35]; therefore, it serves as a robust model to study erythroid terminal differentiation. Erythroid differentiation of c-Kit-enriched BM cells was impaired upon pharmacological inhibition of SPHK1 using a SPHK1-specific inhibitor (SK1-I), as evidenced by the significant reduction in the proportion of Ter119^{+} cells (Figure 3B). Similarly, treatment with SK1-I significantly inhibited erythroid differentiation of MEDEP-BRC5 4 days after EPO induction (Figure 3C), which ultimately resulted in a visible reduction in hemoglobinization (Figure 3D). Therefore, these results indicate that SPHK1 activity and the signaling mediated by S1P are important for terminal erythroid differentiation.

SPHK1 regulates mitochondria content by promoting the expression of BNIP3L/NIX and PINK1

Next, we sought to determine the underlying molecular mechanism by which SPHK1 regulates terminal

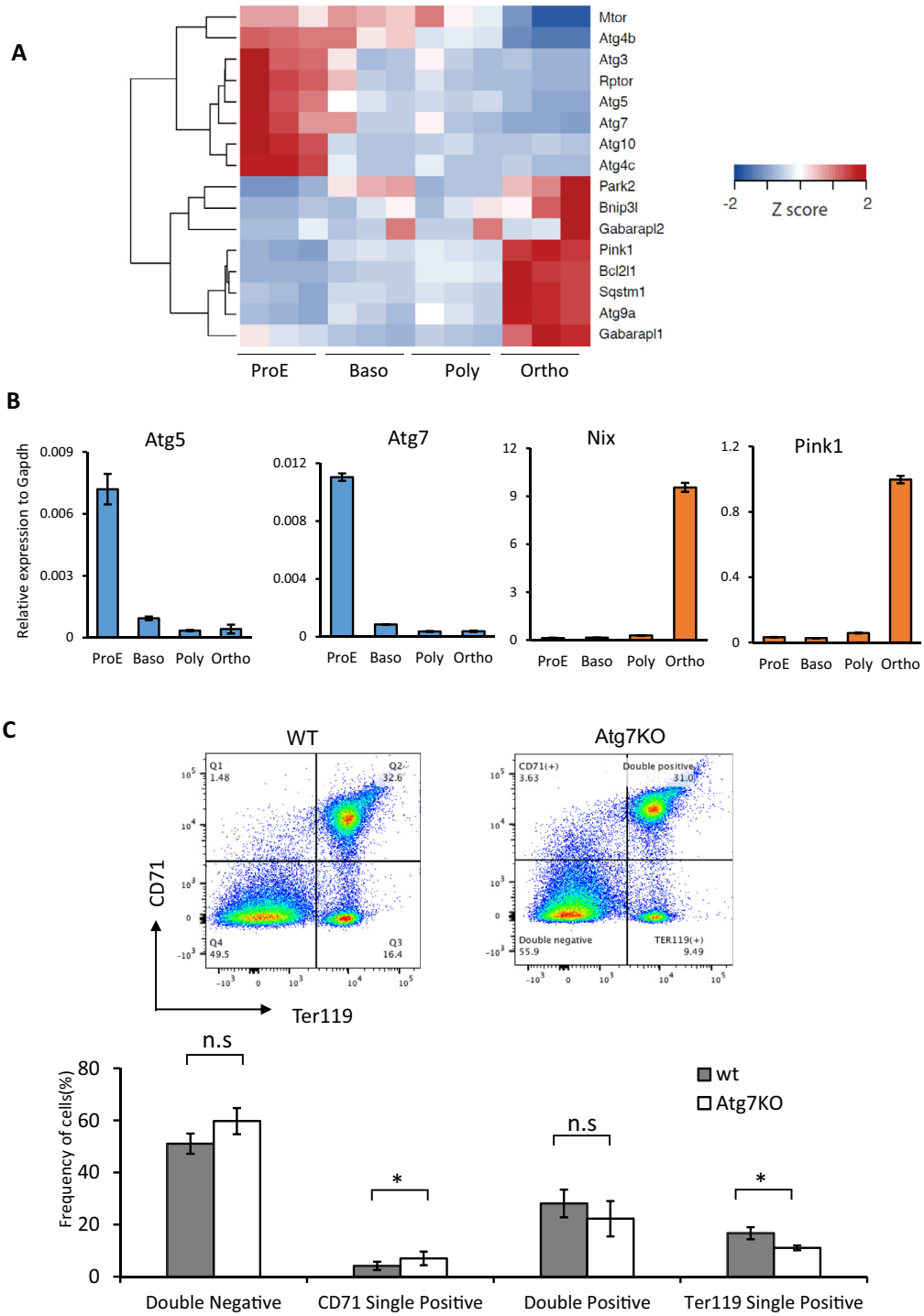

Figure 2. Distinct expression pattern of macroautophagy and mitophagy genes during terminal erythroid differentiation. **(A)** Heat map showing the expression of selected macroautophagy and mitophagy-specific genes. The red, white, and blue colors represent higher than average, close to average, and lower than average expression of a particular gene, respectively, measured by row-standardized *Z* scores. **(B)** qRT-PCR validation of the autophagy gene expressions in various erythroid populations. Error bars indicate the standard error of the mean (SEM) for three independent experiments. **(C)** Representative flow cytometric plots showing the erythroid maturation levels of wild-type (WT) and Atg7-knock-out (KO) mice based on Ter119 and CD71 expression. Quantification of erythroid populations is shown below ($n = 3$ for both WT and Atg7-KO mice)

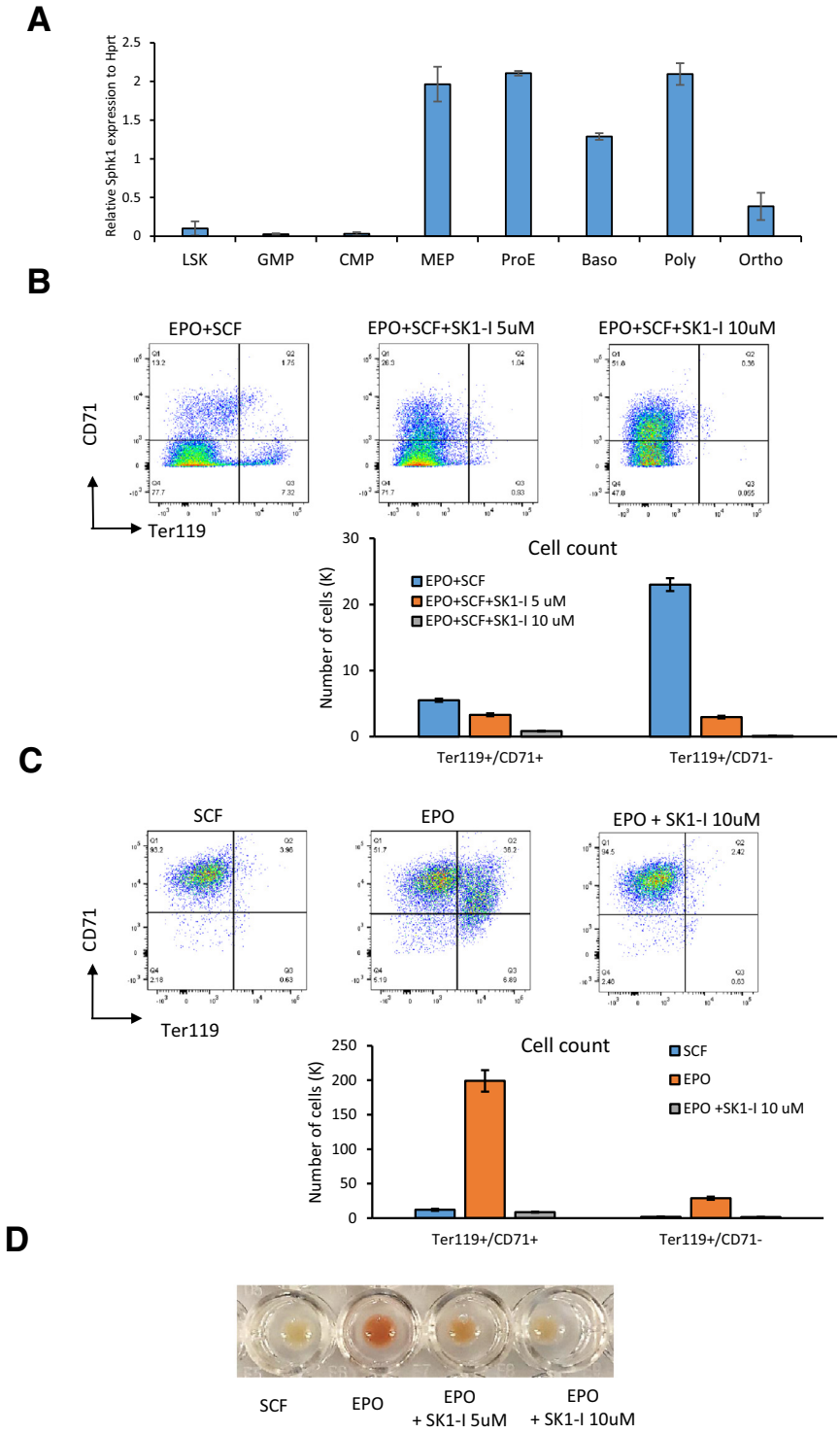

Figure 3. Sphk1 activity is required for erythroid differentiation of primary BM cell and MEDEP cell line culture. **(A)** qRT-PCR analysis of Sphk1 mRNA expression in various hematopoietic cell populations. Error bars indicate the standard error of the mean (SEM) for three independent experiments.. **(B)** Representative flow cytometric plots showing erythroid progression of primary BM cell liquid culture after Sphk1 inhibition (5 or 10 μmol/L) for 7 days. Absolute numbers of cells from the Ter119$^+$/CD71$^+$ and Ter119$^+$/CD71$^-$ populations under each condition are presented. Error bars indicate the standard error of the mean (SEM) for three independent experiments. **(C)** Representative flow cytometric plots showing erythroid progression after 4 days of culture for the MEDEP-BRC5 cell line after Sphk1 inhibition (10 μmol/L). Absolute numbers of cells from the Ter119$^+$/CD71$^+$ and Ter119$^+$/CD71$^-$ populations under each condition are presented. Error bars indicate the standard error of the mean (SEM) for three independent experiments. **(D)** Morphology of 4 days of culture of MEDEP-BRC5 cell line erythroid progression after Sphk1 inhibition (5 or 10 μmol/L). Data shown are representative of three independent experiments.

erythroid differentiation. Regulation of the mitochondrial BH3-only protein BNIP3, which promotes autophagy, is mediated by ceramide (a bioactive sphingolipid) [17,36]. Therefore, we hypothesized that its homolog, BNIP3L/NIX, which is known to regulate mitophagy, is likewise regulated by SPHK1 via the production of the sphingolipid S1P. To address our hypothesis, we measured the expression of *Bnip3l/Nix* and *Pink1* in MEDEP-BRC5 cells upon SPHK1 depletion. Interestingly, SK1-I treatment or shRNA knock-down of *Sphk1* significantly reduced the expression of both *Bnip3l/Nix* and *Pink1* in a dose-dependent manner (Figures 4A and 4B). In contrast, SK1-I treatment or shRNA knock-down of *Sphk1* had no apparent effect on *Atg5* or *Atg7* expression (Figures 4C and 4D). Therefore, these findings suggest that SPHK1/S1P functions during terminal erythroid differentiation to facilitate mitophagy, but not ATG5/7-mediated autophagy, by promoting the expression of *Bnip3l/Nix* and *Pink1*.

In further support of our hypothesis, SK1-I treatment of primary erythroblast cultures (derived from $PhAM^{excised}$ mice) led to an accumulation of mitochondria in $Ter119^+/CD71^+$ erythroid cells (Figure 4E), as shown by the increase in mito-Dendra2 fluorescence intensity following SPHK1 inhibition. Furthermore, we observed a significant increase in TMRE intensity of the erythroid cells ($Ter119^+/CD71^+$) upon SPHK1 inhibition (Figure 4F). Therefore, these findings support the role of SPHK1/S1P in regulating functional mitochondria content, possibly via BNIP3L/NIX and PINK1, during terminal erythroid differentiation.

SPHK1 inhibition disrupts PINK1-p62 mediated mitophagy

To investigate how SPHK1 activity affects mitochondria clearance, we examined the PINK1-p62 axis upon SPHK1 inhibition given that PINK1 activity and its localization to mitochondria not only regulate the clustering of depolarized mitochondria, but also facilitate the subsequent recruitment of the autophagic adaptor p62/SQSTM1 to mediate mitochondria clearance [37,38].

After 7 days of primary erythroid liquid culture, we specifically isolated the late erythroblast ($Ter119^+/CD71^-$) population, a stage when expression of *Pink1* and *p62/SQSTM1* is markedly increased (Figure 2A). Interestingly, under control conditions, PINK1 and p62 are both recruited to mitochondria, which exhibit perinuclear colocalization with PINK1 and p62 (Figure 5A). However, upon SPHK1 inhibition, a reduction in PINK1 is observed (Figure 5B), which is consistent with the decreased *Pink1* mRNA expression upon SPHK1 inhibition (Figure 4A). Moreover, we also observed that SPHK1 inhibition compromises the recruitment of p62 to mitochondria (Figure 5B). Therefore, our findings suggest that the decrease in PINK1 expression upon SPHK1 inhibition subsequently impairs the recruitment of p62 to the mitochondria, which ultimately results in compromised mitochondria clearance and impaired erythroid maturation.

Supplementation of exogenous S1P promotes terminal erythroid differentiation

Given the role of SPHK1/S1P in driving terminal erythroid differentiation, we next assessed the utility of exogenous S1P supplementation for in vitro RBC production. Supplementing murine primary BM erythroid cell cultures with exogenous S1P resulted in a significant increase in the proportion of $Ter119^+$ erythroid cells (Figure 6A). Likewise, exogenous S1P supplementation also significantly increased the $Ter119^+$ fraction in the MEDEP-BRC5 cell line (Figure 6B). Therefore, exogenous S1P supplementation facilitates RBC production in vitro by promoting terminal erythroid differentiation.

Our data demonstrate that SPHK1 activity in erythroid cells promotes terminal erythroid differentiation through the regulation of mitophagy.

Discussion

Our findings uncover the novel role of sphingolipid signaling to modulate key mitophagy genes (i.e., Pink1 and Nix/Bnip3l) that regulate terminal erythroid differentiation. We first reveal that terminal erythroid differentiation entails a progressive reduction in functional mitochondria content. More importantly, we show that macroautophagy factors and key mediators of mitophagy are distinctly expressed during the course of terminal erythroid differentiation. Surprisingly, the expression of macroautophagy factors (Atg5, Atg7, etc.) during the early stages of terminal erythroid differentiation corresponds with the upregulation of genes associated with cell cycle, ribosome biogenesis, and DNA metabolism [28]. In contrast, the expression of key mediators of mitophagy (Pink1, Parkin, Nix/Bnip3l, etc.) during the late stages of terminal erythroid differentiation corresponds to an increased expression of genes associated with macromolecule catabolism and apoptosis [28]. This suggests that macroautophagy may be primarily involved in supporting cell proliferation, rather than mitochondria clearance, during the early stages of terminal erythroid differentiation, after which specialized organelle clearance mechanisms (e.g. mitophagy) and associated catabolic activities are induced to facilitate late-stage terminal erythroid differentiation. Therefore, the progressive reduction in mitochondria observed during terminal erythroid differentiation is directed by distinct, transcriptionally regulated programs.

Given the distinct transcription expression pattern observed and the partially impaired erythropoiesis in ATG7-deficient mice, we postulate that mitochondria clearance during the late stages of terminal erythroid differentiation involves a mode of mitophagy that is independent of Atg7 regulation. Interestingly, recent

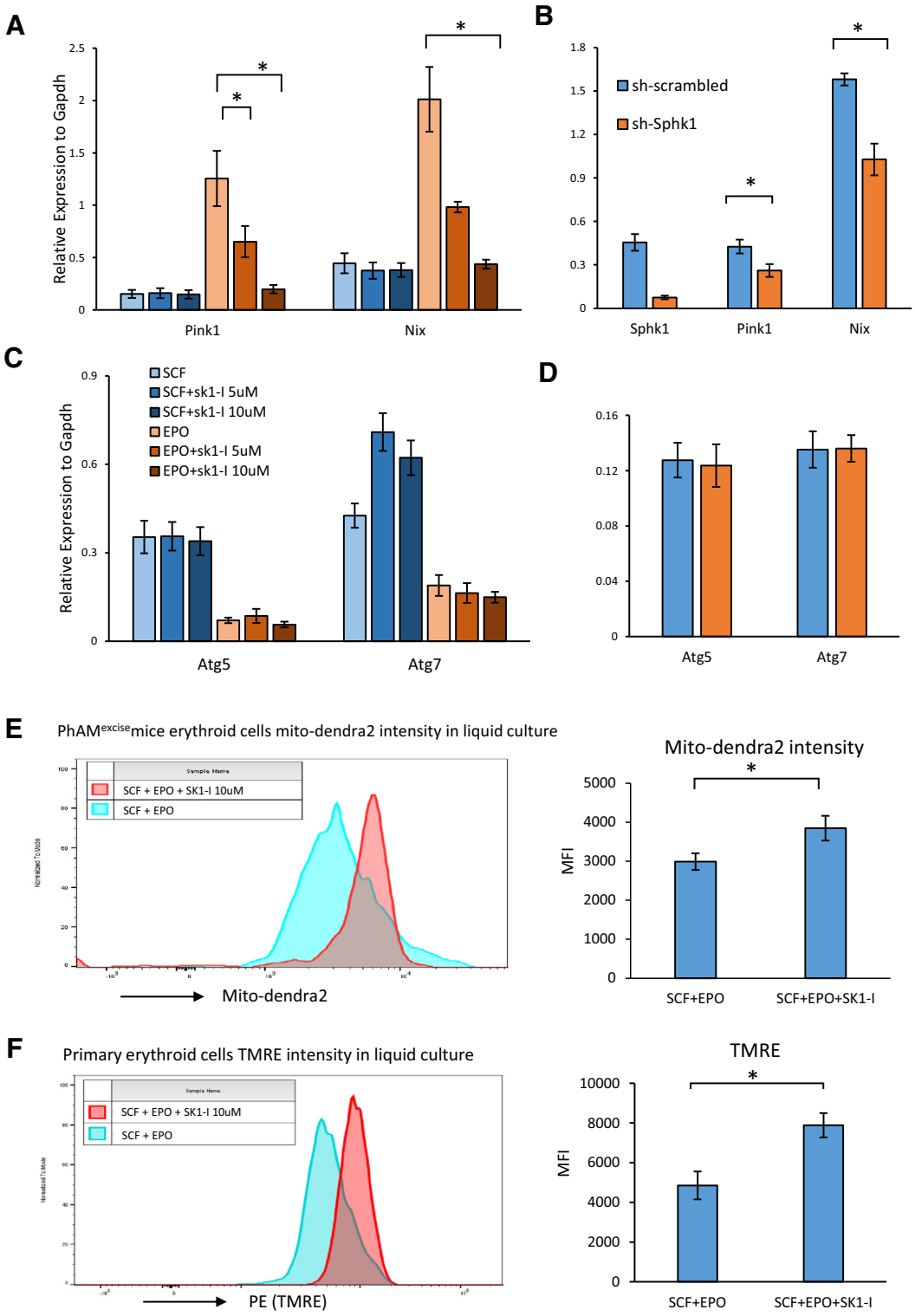

Figure 4. Sphk1 regulates mitophagy genes and modulates mitochondria clearance during terminal erythroid differentiation. **(A,B)** qRT-PCR analysis of Nix and Pink1 mRNA expression after **(A)** Sphk1 inhibition and **(B)** shRNA knock-down of Sphk1 in the MEDEP-BRC5 cell line. **(C,D)** qRT-PCR analysis of Atg5 and Atg7 mRNA expression after **(C)** Sphk1 inhibition and **(D)** sh-RNA knock-down of Sphk1 in the MEDEP-BRC5 cell line. **(E)** Dendra2 fluorescence intensity of the Ter119^{+}/CD71^{+} population in BM cells isolated from PhAM^{excise} mice in liquid culture after Sphk1 inhibition. **(F)** TMRE staining of the Ter119^{+}/CD71^{+} population in BM cells isolated from wild-type (WT) mice in liquid culture after Sphk1 inhibition. Error bars indicate the standard error of the mean (SEM) for three independent experiments. *$p < 0.05$, two-tailed unpaired t test for all experiments.

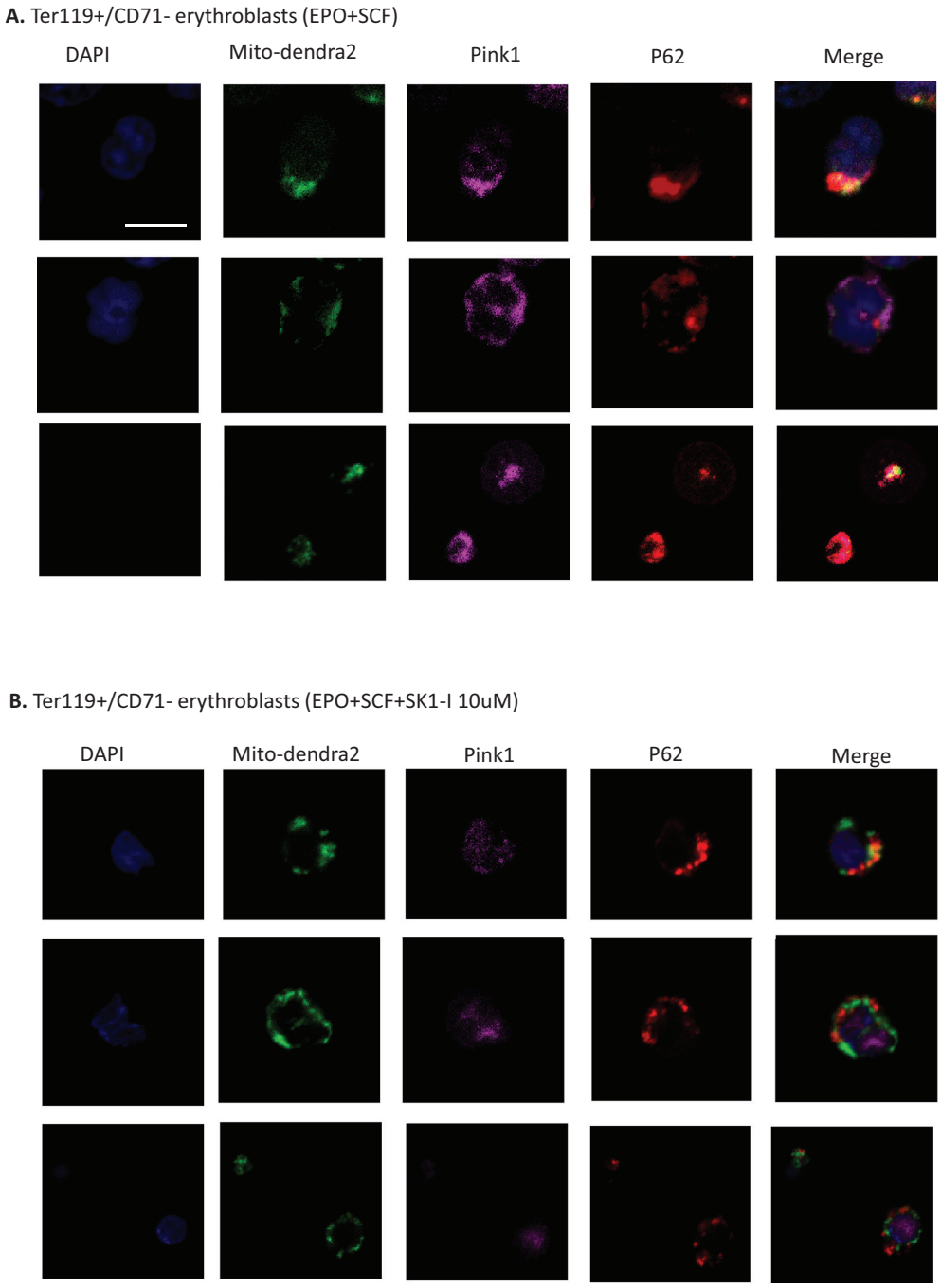

Figure 5. Pharmacological inhibition of Sphk1 disrupts Pink1-p62 mediated mitophagy. **(A,B)** Ter119^{+}/CD71^{-} late erythroblasts are sorted onto the slides after liquid culture of primary BMs cells supplemented with EPO and SCF with **(B)** and without **(A)** 10 μmol/L SK1-I cotreatment for 7 days. Cells were then fixed and analyzed for colocalization between mito-dendra2, Pink1, and p62. Scale bars, 10 μm.

studies reported that Atg9a can target mitochondria and form autophagosomes in the absence of LC3 [39,40]. In agreement, we observed upregulation of Atg9a during the late stages of terminal erythroid differentiation (Figure 2A). We also show that terminal erythroid differentiation also correlated with upregulation of Nix/Bnip3l (Figure 2B), which has previously been implicated in mitophagy during erythroid maturation [13,14]. Mechanistically, Nix was reported to prime mitochondria for autophagic recognition [41] and interact directly with gamma-aminobutyric acid type A (GABA[A]) receptor-associated protein (GABARAP), which is involved in autophagy [42]. Therefore, mitophagy during the late stages of terminal

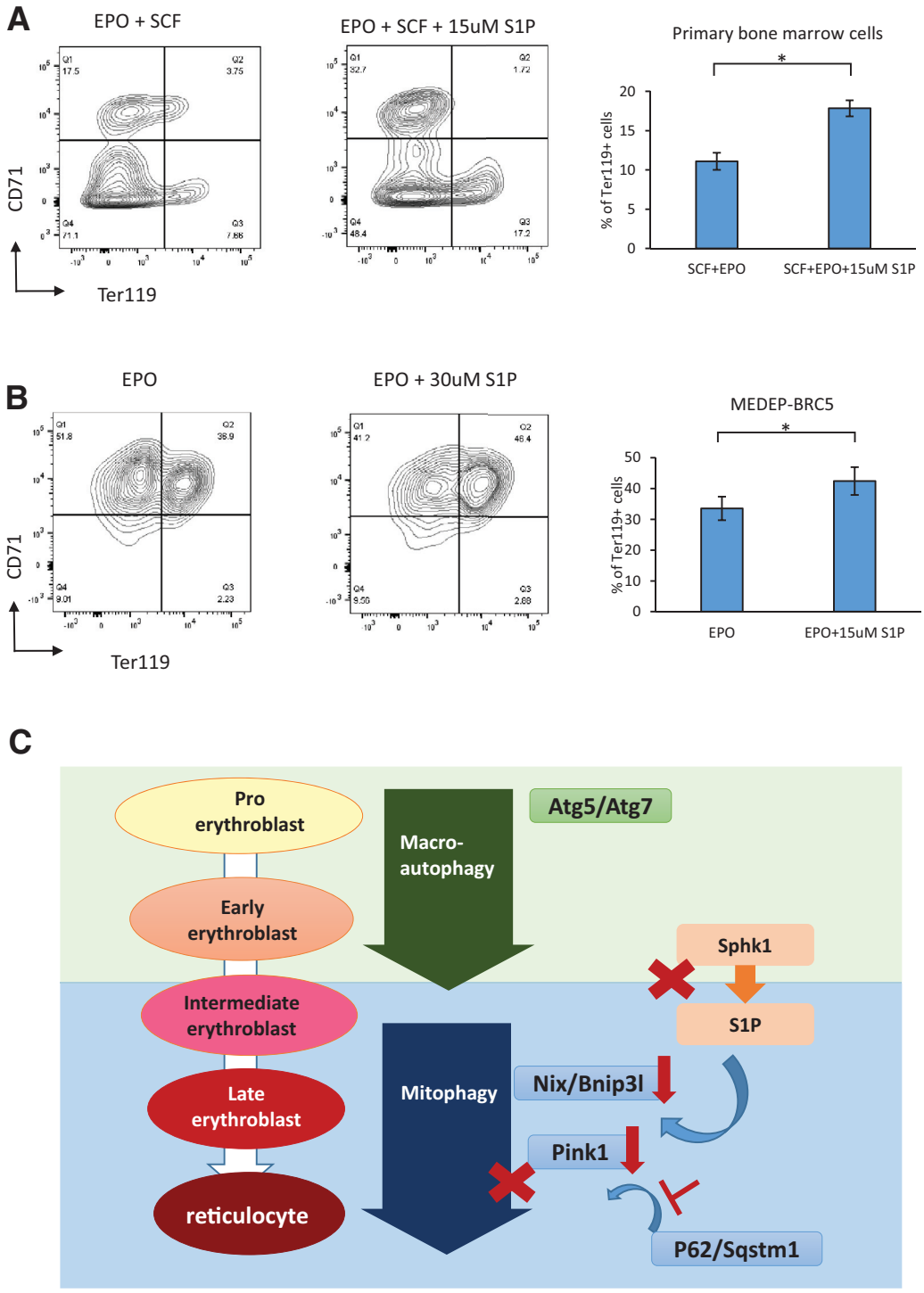

Figure 6. Exogenous S1P administration facilitates terminal erythroid differentiation. **(A)** Representative flow cytometric plots showing erythroid progression of liquid culture of murine BM cells (with SCF and EPO) upon cotreatment of exogenous S1P for 7 days. **(B)** Representative flow cytometric plots showing erythroid progression of the MEDEP-BRC5 cell line culture upon administration of exogenous S1P for 4 days. Error bars indicate the standard error of the mean (SEM) for three independent experiments. $*p < 0.05$, two-tailed unpaired t test for all experiments. **(C)** Schematic model for Sphk1 and S1P signaling and their inhibition effects in terminal erythroid differentiation involving the modulation of mitophagy activities through the regulation of Nix and Pink1 expression.

erythroid differentiation appears to be mediated via an Atg7-independent mechanism.

It was previously reported that ceramide inhibits CFU-E colony formation and that this effect is reversed by the ceramide antagonist S1P [43]. Consistent with the anti-apoptotic role of S1P [19], we observed that SPHK1 inhibition results in increased apoptosis of erythroid cells in vitro (Supplementary Figure E1, online only, available at www.exphem.org). Apoptosis is associated with elevated cellular ROS levels (i.e., oxidative stress) [44], which decrease in the late stage of terminal differentiation (Figure 1D) and have been shown to negatively regulate terminal erythropoiesis [45]. More importantly, our data strongly suggest that, during terminal erythroid differentiation, mitochondria clearance, which effectively mitigates the elevated ROS level, is regulated by the activity of SPHK1- and S1P-mediated signaling. In support of this hypothesis, we confirmed that Sphk1 is preferentially expressed in the erythroid lineage. Importantly, we demonstrated that disruption of sphingolipid signaling led to reduced expression of the key mitophagy genes Pink1 and Nix/Bnip3l, which likely accounts for the impaired mitochondria clearance and terminal erythropoiesis observed. More specifically, the role of Nix/Bnip3l in the regulation of mitophagy in erythropoiesis has been validated in knock-out mice models [14]. We further show that reduced Pink1 expression upon Sphk1 inhibition results in suppressed p62 recruitment to mitochondria for mitochondrial degradation in late erythroblasts. Therefore, the increased apoptotic erythroid cells upon Sphk1 inhibition is possibly due to elevated ROS levels resulting from impaired mitochondria clearance, which is required for optimal erythroid differentiation. In further support, we show that supplementing exogenous S1P facilitated terminal erythroid differentiation. Therefore, sphingosine signaling involving S1P regulates mitophagy during terminal erythroid differentiation, although it remains unclear how S1P signaling leads to transcriptional upregulation of these mitophagy-associated genes identified.

Our results demonstrate that sphingolipid signaling involving Sphk1-derived S1P promotes terminal differentiation through the regulation of Pink1-p62- and Nix/Bnip3l-mediated mitophagy (Figure 6C) and provide insight into potentially addressing the demand for the large-scale in vitro production of RBCs.

Acknowledgments

We thank Dr. Takayoshi Matsumura, Dr. Ayako Nakamura-Ishizu, and Dr. Mitsuhiro Endo for advice and suggestions on this work and A'Qilah Banu Bte Abdul Majeed and Kaoru Yoshikawa for technical assistance.

TS is a National Medical Research Council (NMRC) of Singapore Translational Research Investigator (STaR) Award Investigator.

Conflict of interest disclosure

The authors declare no competing interests.

References

1. Dzierzak E, Philipsen S. Erythropoiesis: development and differentiation. Cold Spring Harb Perspect Med. 2013;3:a011601.
2. Tsiftsoglou AS, Vizirianakis IS, Strouboulis J. Erythropoiesis: model systems, molecular regulators, and developmental programs. IUBMB Life. 2009;61:800–830.
3. Manwani D, Bieker JJ. The erythroblastic island. Curr Top Dev Biol. 2008;82:23–53.
4. Palis J. Primitive and definitive erythropoiesis in mammals. Front Physiol. 2014;5:3.
5. Haase VH. Hypoxic regulation of erythropoiesis and iron metabolism. Am J Physiol Renal Physiol. 2010;299:F1–F13.
6. Mankelow TJ, Griffiths RE, Trompeter S, et al. The ins and outs of reticulocyte maturation revisited: The role of autophagy in sickle cell disease. Autophagy. 2016;12:590–591.
7. Zhang J, Wu K, Xiao X, et al. Autophagy as a regulatory component of erythropoiesis. Int J Mol Sci. 2015;16:4083–4094.
8. Yang C, Suda T. Hyperactivated mitophagy in hematopoietic stem cells. Nat Immunol. 2018;19:2–3.
9. Lazarou M, Jin SM, Kane LA, Youle RJ. Role of PINK1 binding to the TOM complex and alternate intracellular membranes in recruitment and activation of the E3 ligase Parkin. Dev Cell. 2012;22:320–333.
10. Mortensen M, Ferguson DJ, Edelmann M, et al. Loss of autophagy in erythroid cells leads to defective removal of mitochondria and severe anemia in vivo. Proc Natl Acad Sci USA. 2010;107:832–837.
11. Joshi A, Kundu M. Mitophagy in hematopoietic stem cells: the case for exploration. Autophagy. 2013;9:1737–1749.
12. Kundu M, Lindsten T, Yang CY, et al. Ulk1 plays a critical role in the autophagic clearance of mitochondria and ribosomes during reticulocyte maturation. Blood. 2008;112:1493–1502.
13. Novak I, Kirkin V, McEwan DG, et al. Nix is a selective autophagy receptor for mitochondrial clearance. EMBO Rep. 2010;11:45–51.
14. Sandoval H, Thiagarajan P, Dasgupta SK, et al. Essential role for Nix in autophagic maturation of erythroid cells. Nature. 2008;454:232–235.
15. Honda S, Arakawa S, Nishida Y, Yamaguchi H, Ishii E, Shimizu S. Ulk1-mediated Atg5-independent macroautophagy mediates elimination of mitochondria from embryonic reticulocytes. Nat Commun. 2014;5:4004.
16. Zhang J, Randall MS, Loyd MR, et al. Mitochondrial clearance is regulated by Atg7-dependent and -independent mechanisms during reticulocyte maturation. Blood. 2009;114:157–164.
17. Young MM, Kester M, Wang HG. Sphingolipids: regulators of crosstalk between apoptosis and autophagy. J Lipid Res. 2013;54:5–19.
18. Maiuri MC, Zalckvar E, Kimchi A, Kroemer G. Self-eating and self-killing: crosstalk between autophagy and apoptosis. Nat Rev Mol Cell Biol. 2007;8:741–752.
19. Cuvillier O, Pirianov G, Kleuser B, et al. Suppression of ceramide-mediated programmed cell death by sphingosine-1-phosphate. Nature. 1996;381:800–803.
20. Hannun YA, Obeid LM. Principles of bioactive lipid signaling: lessons from sphingolipids. Nat Rev Mol Cell Biol. 2008;9:139–150.
21. Pyne NJ, Ohotski J, Bittman R, Pyne S. The role of sphingosine 1-phosphate in inflammation and cancer. Adv Biol Regul. 2014;54:121–129.
22. Pappu R, Schwab SR, Cornelissen I, et al. Promotion of lymphocyte egress into blood and lymph by distinct sources of sphingosine-1-phosphate. Science. 2007;316:295–298.

23. Yang L, Yatomi Y, Miura Y, Satoh K, Ozaki Y. Metabolism and functional effects of sphingolipids in blood cells. Br J Haematol. 1999;107:282–293.
24. Maceyka M, Sankala H, Hait NC, et al. SphK1 and SphK2, sphingosine kinase isoenzymes with opposing functions in sphingolipid metabolism. J Biol Chem. 2005;280:37118–37129.
25. Ksiazek M, Chacinska M, Chabowski A, Baranowski M. Sources, metabolism, and regulation of circulating sphingosine-1-phosphate. J Lipid Res. 2015;56:1271–1281.
26. Xiong Y, Yang P, Proia RL, Hla T. Erythrocyte-derived sphingosine 1-phosphate is essential for vascular development. J Clin Invest. 2014;124:4823–4828.
27. Pronk CJ, Rossi DJ, Mansson R, et al. Elucidation of the phenotypic, functional, and molecular topography of a myeloerythroid progenitor cell hierarchy. Cell Stem Cell. 2007;1:428–442.
28. An X, Schulz VP, Li J, et al. Global transcriptome analyses of human and murine terminal erythroid differentiation. Blood. 2014;123:3466–3477.
29. Trapnell C, Pachter L, Salzberg SL. TopHat: discovering splice junctions with RNA-Seq. Bioinformatics. 2009;25:1105–1111.
30. Anders S, Pyl PT, Huber W. HTSeq–a Python framework to work with high-throughput sequencing data. Bioinformatics. 2015;31:166–169.
31. Chen K, Liu J, Heck S, Chasis JA, An X, Mohandas N. Resolving the distinct stages in erythroid differentiation based on dynamic changes in membrane protein expression during erythropoiesis. Proc Natl Acad Sci U S A. 2009;106:17413–17418.
32. van Wijk R, van Solinge WW. The energy-less red blood cell is lost: erythrocyte enzyme abnormalities of glycolysis. Blood. 2005;106:4034–4042.
33. de Almeida MJ, Luchsinger LL, Corrigan DJ, Williams LJ, Snoeck HW. Dye-independent methods reveal elevated mitochondrial mass in hematopoietic stem cells. Cell Stem Cell. 2017;21:725–729.e4.
34. Pham AH, McCaffery JM, Chan DC. Mouse lines with photoactivatable mitochondria to study mitochondrial dynamics. Genesis. 2012;50:833–843.
35. Hiroyama T, Miharada K, Sudo K, Danjo I, Aoki N, Nakamura Y. Establishment of mouse embryonic stem cell-derived erythroid progenitor cell lines able to produce functional red blood cells. PLoS One. 2008;3:e1544.
36. Mammucari C, Milan G, Romanello V, et al. FoxO3 controls autophagy in skeletal muscle in vivo. Cell Metab. 2007;6:458–471.
37. Geisler S, Holmstrom KM, Skujat D, et al. PINK1/Parkin-mediated mitophagy is dependent on VDAC1 and p62/SQSTM1. Nat Cell Biol. 2010;12:119–131.
38. Lee JY, Nagano Y, Taylor JP, Lim KL, Yao TP. Disease-causing mutations in Parkin impair mitochondrial ubiquitination, aggregation, and HDAC6-dependent mitophagy. J Cell Biol. 2010;189:671–679.
39. Ding WX, Yin XM. Mitophagy: mechanisms, pathophysiological roles, and analysis. Biol Chem. 2012;393:547–564.
40. Itakura E, Kishi-Itakura C, Koyama-Honda I, Mizushima N. Structures containing Atg9A and the ULK1 complex independently target depolarized mitochondria at initial stages of Parkin-mediated mitophagy. J Cell Sci. 2012;125:1488–1499.
41. Ding WX, Ni HM, Li M, et al. Nix is critical to two distinct phases of mitophagy, reactive oxygen species–mediated autophagy induction and Parkin-ubiquitin-p62-mediated mitochondrial priming. J Biol Chem. 2010;285:27879–27890.
42. Schwarten M, Mohrluder J, Ma P, et al. Nix directly binds to GABARAP: a possible crosstalk between apoptosis and autophagy. Autophagy. 2009;5:690–698.
43. Dallalio G, North M, Worden BD, Means Jr RT. Inhibition of human erythroid colony formation by ceramide. Exp Hematol. 1999;27:1133–1138.
44. Circu ML, Aw TY. Reactive oxygen species, cellular redox systems, and apoptosis. Free Radic Biol Med. 2010;48:749–762.
45. Zhao B, Mei Y, Yang J, Ji P. Erythropoietin-regulated oxidative stress negatively affects enucleation during terminal erythropoiesis. Exp Hematol. 2016;44:975–981.

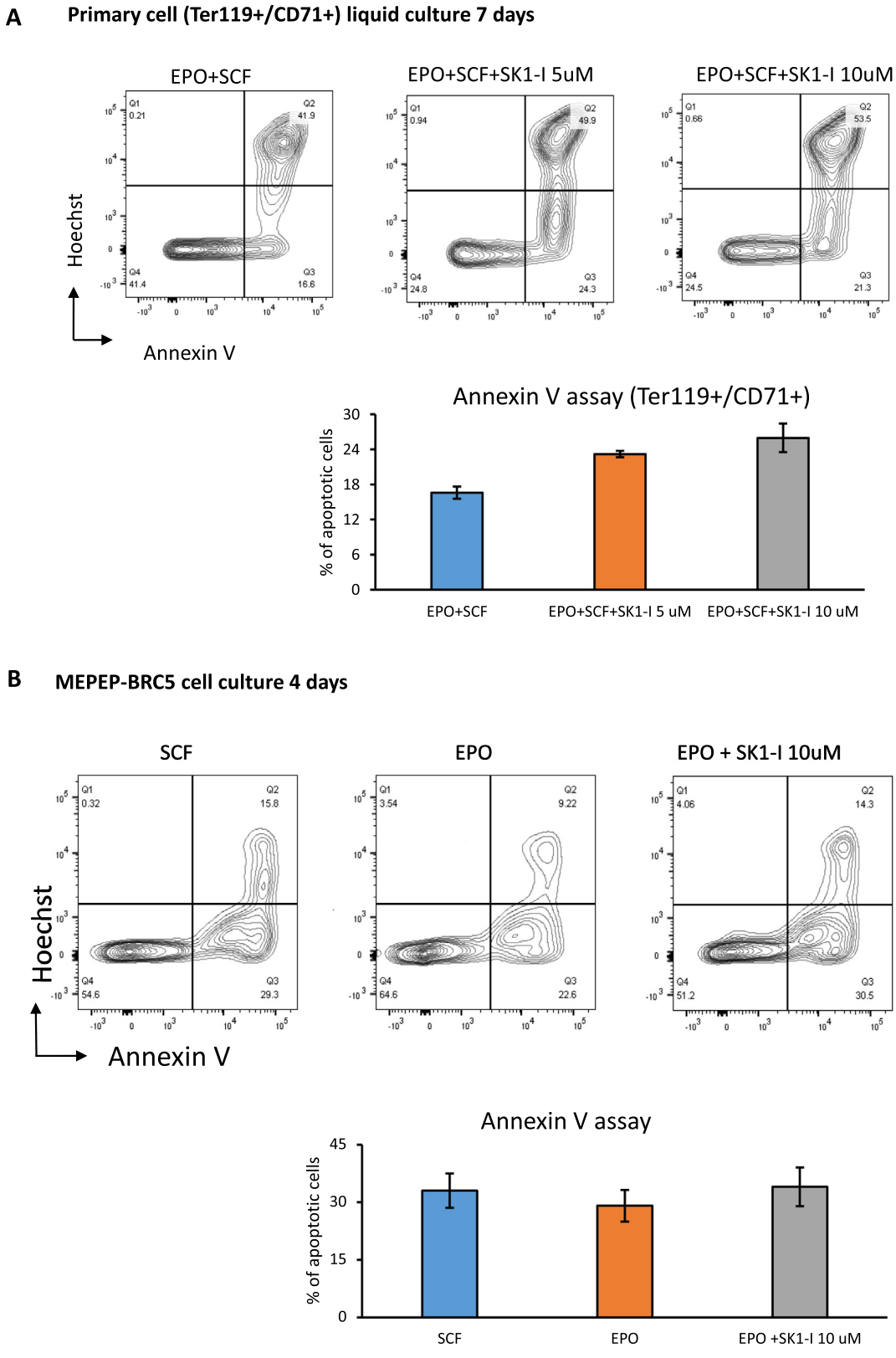

Figure E1. Pharmacological inhibition of Sphk1 moderately affects apoptosis in **(A)** primary cell ($Ter119^{+}/CD71^{+}$) liquid culture after 7 days and **(B)** MEDEP-BRC5 cell culture after 4 days. Percentage of apoptotic cells (annexin V^{+}/$Hoechst^{-}$) are presented. Error bars indicate the standard error of the mean for three independent experiments.